

# Glass Formation in a Periodic Long-Range Josephson Array

P. Chandra<sup>1</sup>, M.V. Feigelman<sup>2</sup> and L.B. Ioffe<sup>2,3</sup>

<sup>1</sup>NEC Research Institute, 4 Independence Way, Princeton NJ 08540

<sup>2</sup>Landau Institute for Theoretical Physics, Moscow, RUSSIA

<sup>3</sup>Department of Physics, Rutgers University, Piscataway, NJ 08855

We present an analytic study of a dynamical instability in a periodic long-range Josephson array frustrated by a weak transverse field. This glass transition is characterized by a diverging relaxation time and a jump in the Edwards-Anderson order parameter; it is *not* accompanied by a coinciding static transition.

Glass formation in the *absence* of intrinsic disorder is a long-standing problem. Although vitrification is ubiquitous, a minimalist microscopic model of this phenomenon remains the subject of active discussion. [1] Because glass formation is a dynamical transition that is not necessarily accompanied by a static one, it lies outside the framework of the Landau theory. Furthermore this glass transition leads to a low-temperature phase with broken ergodicity *without* the selection of a *unique* state. A successful phenomenological theory should describe the “partitioning” of phase space below the transition temperature ( $T_G$ ) into an exponential number of metastable states; specifically it should explain how the system becomes “stuck” at  $T_G$  in one of these states that is separated from the others by barriers that scale with the system size.

Unfortunately a basic theory of glass formation has not yet been found. Several microscopic non-random models have been proposed; most were studied via a mapping to disordered systems [2]. Recently possible glassiness in the absence of disorder has been studied in a periodic long-range Josephson array using a direct, analytic approach [3]; furthermore this system may be realized experimentally. An analysis of its static behavior indicates a first-order transition into a low-temperature phase characterized by an extensive number of states separated by infinite barriers. In this Letter we continue the study of this system and show that it displays a true dynamical instability that *precedes* the static transition, as expected in a glass. [1]

The proposed array is a stack of two mutually perpendicular sets of  $N$  parallel wires with Josephson junctions at each node (Figure 1) that is placed in an external transverse field. The classical thermodynamic variables of this system are the superconducting phases associated with each wire. Here we shall assume that the Josephson couplings are sufficiently small so that the induced fields are negligible in comparison with  $H$ . We can therefore describe the array by the Hamiltonian

$$\mathcal{H} = - \sum_{m,n}^{2N} s_m^* \mathcal{J}_{mn} s_n \quad (1)$$

where  $\mathcal{J}_{mn}$  is the coupling matrix

$$\hat{\mathcal{J}} = \begin{pmatrix} 0 & \hat{J} \\ \hat{J}^\dagger & 0 \end{pmatrix} \quad (2)$$

with  $J_{jk} = \frac{J_0}{\sqrt{N}} \exp(2\pi i \alpha j k / N)$  and  $1 \leq (j, k) \leq N$  where  $j(k)$  is the index of the horizontal (vertical) wires;  $s_m = e^{i\phi_m}$  where the  $\phi_m$  are the superconducting phases of the  $2N$  wires. Here we have introduced the flux per unit strip,  $\alpha = NHl^2/\phi_0$ , where  $l$  is the inter-node spacing and  $\phi_0$  is the flux quantum; the normalization has been chosen so that  $T_G$  does not scale with  $N$ .

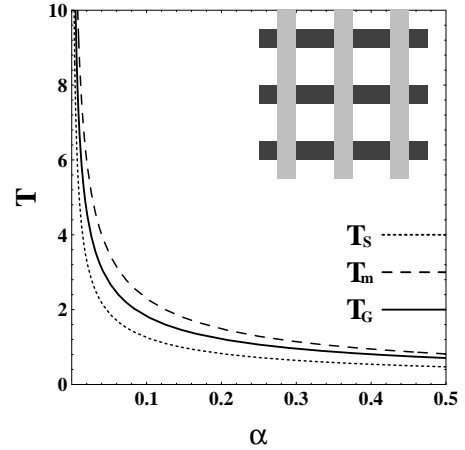


Fig 1. The phase diagram of the array (inset) where  $T_G$  indicates the temperature associated with the dynamical instability discussed in this Letter,  $T_S$  is the speculated equilibrium transition temperature and  $T_m$  is the “superheating” temperature where the low-temperature metastable states cease to exist.

Because every horizontal (vertical) wire is linked to every vertical (horizontal) wire, the number of nearest neighbors ( $z$ ) in this model is  $N$ ; we can therefore study it with a mean-field approach. For  $\frac{1}{N} \ll \alpha < 1$  the number of low-temperature metastable solutions is extensive [3]. Furthermore this degeneracy develops simultaneously with the instability of the paramagnetic phase; at this temperature interactions do not favor a particular

state and, because  $z \sim N$ , the barriers separating these low-temperature metastable solutions are effectively infinite. The static response displays *no* soft mode instability but indicates a jump in the Edwards-Anderson order parameter in the vicinity of  $T_0 = \frac{J_0}{\sqrt{\alpha}}$ .

Before presenting our quantitative treatment of the dynamical behavior of this array, we discuss the qualitative picture of the glass transition that emerges from our results (cf. Fig. 1). As  $T$  approaches  $T_m^+$ , where  $T_m^+ \sim T_0$ , there appear a number of metastable states in addition to the paramagnetic free-energy minimum; most likely they are energetically unfavorable and thus do not “trap” the system upon cooling from high temperatures. As  $T \rightarrow T_G^+$ , the paramagnetic minimum is “subdivided” into an extensive number of degenerate metastable states separated by effectively infinite barriers, and the system is dynamically localized into one of them. Qualitatively, in the interval  $T_m > T > T_G$  there appear many local minima in the vicinity of the paramagnetic state separated by *finite* barriers; these barriers increase continuously and become infinite at  $T = T_G$ . Each of these minima is characterized by a finite “site magnetization”  $m_i = \langle s_i \rangle_T$  where “site” refers to a wire. When  $T > T_G$  thermal fluctuations average over many states so that  $\langle m_i \rangle \equiv 0$ . At  $T = T_G$  the system is localized in one metastable state and there is an associated jump in the Edwards-Anderson order parameter, ( $q = \frac{1}{N} \sum_i \langle m_i \rangle^2$ ). The low-temperature phase is characterized by a finite  $q$  and by the presence of a memory,  $\lim_{t' \rightarrow \infty} \Delta(t, t') \neq 0$  where  $\Delta(t, t')$  is the anomalous response. We expect that at  $T = T_G$ , the metastable states are degenerate and thus there can be no thermodynamic selection. However at lower temperatures interactions will probably break this degeneracy and select a subset of this manifold; then we expect an ( $t \rightarrow \infty$ ) equilibrium first-order transition ( $T_S$ ) which should be accompanied by a jump in the local magnetization. In order to observe this transition at  $T_S$  the array must be equilibrated on a time-scale ( $t_W$ ) longer than that ( $t_A$ ) necessary to overcome the barriers separating its metastable states;  $t_A$  scales exponentially with the number of wires in the array. Thus the equilibrium transition at  $T_S$  is observable *only* if  $t_W \rightarrow \infty$  *before* the thermodynamic limit ( $N \rightarrow \infty$ ) is taken; in the opposite order of limits only the dynamical transition occurs.

We now begin a more quantitative analysis of the dynamic instability in this periodic array. Because our focus is on the long-time behavior of this system, we expect the details of the single-spin dynamics to be irrelevant; we therefore choose to study the simplest form, namely that of soft spins with Langevin relaxational dynamics. More specifically, we introduce a “potential”,  $V(S_i) = V_0(|S|^2 - 1)^2$ , at each wire which constrains the magnitude of each spin,  $|S_i| \approx 1$ , and assume the equations of motion

$$\tau_b \dot{S}_i = -\frac{1}{T} \frac{\partial(\mathcal{H} + V)}{\partial S_i} + \zeta_i \quad (3)$$

$$\langle \zeta_i(t) \zeta_j(t') \rangle = 2\tau_b \delta(t - t') \quad (4)$$

where  $\tau_b$  is a microscopic time-scale. The dynamics (3) reproduces the dynamics of the overdamped Josephson junctions with individual resistance  $R$  if  $\tau_b = \frac{\hbar^2}{(2e)^2 RT}$  and  $V_0 \rightarrow \infty$ . In order to average the solution of (3) over the thermal noise,  $\zeta$ , we use a generating functional. For example, the average supercurrent in the array is given by

$$\langle I_{ij} \rangle = \int I_{ij} \exp \mathcal{A}[S, \hat{S}] \mathcal{D}S \mathcal{D}\hat{S}. \quad (5)$$

Here the current  $I_{ij} = \left(\frac{2e}{\hbar c}\right) \text{Im} S_i^* J_{ij} S_j$  and the action is

$$\mathcal{A} = \int dt \left[ \hat{S} \left( \tau_b \dot{S} + \frac{1}{T} \frac{\partial(\mathcal{H} + V)}{\partial S} \right) + \tau_b \hat{S}^2 \right] \quad (6)$$

where we have not included the terms that arise from the Jacobian since they do not affect the long-time response. [5–7]

We perform our calculations by resumming the terms in the  $\frac{\hbar}{T}$  expansion of (5) which are leading order in  $\frac{1}{N}$ ; this is a dynamical analogue of the high-temperature series expansion previously used to study the static behavior of this array. [3] The crucial ingredients of this technique are the response ( $G_{mn}(t, t') = \langle s_m(t) \hat{s}_n(t') \rangle$ ) and the correlation ( $C_{mn}(t, t') = \langle s_m(t) s_n^*(t') \rangle$ ) functions. For  $T > T_G$ , these depend *only* on the time-differences and thus can be related by the Fluctuation-Dissipation Theorem

$$G_{ij}(t - t') = -\frac{\partial D_{ij}(t - t')}{\partial t} \theta(t - t') \quad (7)$$

The leading diagrams (in  $\frac{1}{N}$ ) for  $G_{ij}(t - t')$  are displayed in Fig. 2a. The presence of the “constraining potential”  $V$  in the action (6) results in finite higher-order irreducible single-site spin correlations, which play the role of interaction vertices in this diagrammatic technique. However the corrections to the response function shown in Fig. 2b are small in  $\frac{1}{N}$  in comparison with those in Fig. 2a.

We emphasize that, as in the static case, the single-site response is renormalized; here we consider the local Green’s function ( $\tilde{G}(t - t')$ ) that is irreducible with respect to the  $J_{ij}$  lines. Possible self-energy corrections to  $\tilde{G}(t - t')$  are shown in Fig. 2c and will be discussed below. Summing the geometric series shown in Fig. 2a, we obtain

$$\hat{G}_\omega = \frac{1}{\tilde{G}_\omega^{-1} - \beta^2 (J^\dagger J) \tilde{G}_\omega} \quad (8)$$

for the response function connecting wires of the same type (horizontal/vertical). The matrix  $(J^\dagger J)_{ij}$  depends only on the “distance”  $i - j$  and acquires a simple form

in Fourier space  $(J^\dagger J)_p = (J_0^2/\alpha)\theta(\alpha\pi - |p|)$ ; in this representation the Green function becomes

$$G_\omega(p) = \frac{\theta(\alpha\pi - |p|)}{\tilde{G}_\omega^{-1} - \frac{(\beta J_0)^2}{\alpha}\tilde{G}_\omega} + \frac{\theta(|p| - \alpha\pi)}{\tilde{G}_\omega^{-1}}. \quad (9)$$

The static limit ( $\omega = 0$ ) of  $T\tilde{G}_\omega^{-1}$  coincides with the locator,  $A(T)$ , discussed previously [3]; in the absence of Onsager feedback terms  $\tilde{G}_0^{-1} = 1$ . Therefore we see in (9) that there would be a static instability at  $\tilde{G}_0^{-1} = G_c = \frac{\beta J_0}{\sqrt{\alpha}}$ . For  $\Theta = (T - T_0)/T_0 \gg \sqrt{\alpha}$  all feedback effects are negligible. Here the time-dependence of  $\tilde{G}_\omega^{-1}$  is set by a microscopic time-scale  $\tau_b$  and  $\tilde{G}_b^{-1}(\omega) = \beta A(T) - i\omega\tau_b$ ; inserting this  $\tilde{G}_b^{-1}(\omega)$  into (9) we see that the long-time behavior of  $G_\omega(p)$  is dominated by the first term which results in a long relaxation time  $\tau = (2/\alpha)\tau_b$  where  $a = \beta(A - \frac{J_0^2}{\alpha A}) \approx 2\Theta$ . In this regime the single-site response function is

$$G(t) = \frac{\alpha}{2\tau_b} e^{-t/\tau} \quad t \gg \tau_b. \quad (10)$$

At lower temperatures,  $\Theta \lesssim \sqrt{\alpha}$ , the feedback effects become important; they modify  $\tilde{G}_0^{-1}$  so that it approaches  $G_c$  only asymptotically at  $T \rightarrow 0$  and instead a first-order transition occurs [3]. The retardation of the Onsager terms is also crucial and significantly affects the long-time behavior. Qualitatively the resulting dynamical instability, described below, is due to the time-dependence of the cavity field which itself is determined by single-site susceptibilities; the time-scale associated with the relaxation of  $G(t)$  increases continuously due to feedback through the Onsager terms. Formally the latter introduce an additional frequency-dependent part of the local response

$$\tilde{G}_\omega^{-1} = \tilde{G}_b^{-1}(\omega) - \Sigma_\omega \quad (11)$$

as a self-energy  $\Sigma_\omega$  such that  $\Sigma_0 = 0$  since we have chosen our normalization so that  $\tilde{G}_0^{-1} = \beta A(T)$ .

The on-site self-energy terms (see Fig. 2c) are the simplest for  $\alpha \ll 1$ , and thus we will consider this regime. We focus on the long-time response of this system which is dominated by the first term in (9) when  $\tilde{G}_0^{-1} \approx G_c$ ; its weight is proportional to  $\alpha$  (cf. (10)). Thus in the limit of  $\alpha \ll 1$ , the slowly decaying parts of  $D(t)$  and  $G(t)$  scale with  $\alpha$  and the dominant self-energy contribution contains the minimal number of these functions ( $\Sigma^{(3)}$  in Fig. 2c) and is given by

$$\Sigma_\omega = \Gamma^2 \int D^2(t)G(t) (e^{i\omega t} - 1) dt \quad (12)$$

where  $D$  and  $G$  are single-site correlation and response functions respectively. [4] Here  $\Gamma$  is the four-spin vertex; we neglect its transient time-dependence and approximate it by its static value  $\Gamma = -1$  which is determined by

the high-temperature single-site nonlinear susceptibility  $\chi_3 = -\frac{1}{T^3}$ . The set of equations, (7), (9), (11) and (12), are sufficient to determine the response and the correlation functions of the array.

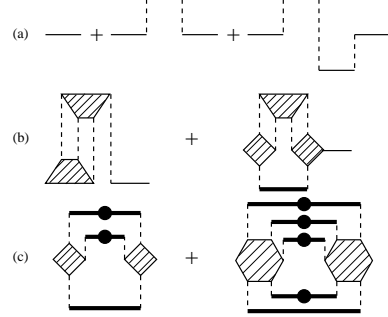


Fig 2. Diagrammatic expansion for the response function  $\hat{G}(t)$ ; the dashed, solid and thick (with dot) lines are the coupling matrix  $\mathcal{J}$ , the single site irreducible ( $\tilde{G}(t)$ ) and the full response (correlation) functions respectively. a. Leading order in  $1/N$ . b. Subleading order in  $1/N$ . c. Leading terms in the expansion for  $\tilde{G}(t)$ ; the first diagram dominates at small  $\alpha$ .

Since we would like to detect a dynamical instability, we only consider the long-time behavior of the response function, i.e.

$$G(t) = \alpha \int \frac{e^{-i\omega t}}{a - 2(\Sigma_\omega + i\omega\tau_b)} \left( \frac{d\omega}{2\pi} \right). \quad (13)$$

We make the ansatz

$$\Sigma_\omega = \frac{i\omega\tau_0/2}{1 - i\omega\tau_1} \quad (14)$$

and show that it solves the system of equations (7,9,11,12); in the process we also obtain the time-scales  $\tau_0$  and  $\tau_1$  controlling the physical response. We have chosen this form of  $\Sigma_\omega$  so that  $\Sigma_0 = 0$  and  $\Sigma(t) \sim \exp(-t/\tau_1)$ . Inserting this ansatz into (13), we obtain response and correlation functions that are simple exponentials for long times; therefore the resulting self-energy (cf. (12)) is also exponential and thus of the same form as the initial ansatz. Equating the parameters of (14) and (12), we find that the condition for self-consistency at  $a \rightarrow a_c$  is

$$\tau_1 = \frac{1}{3} \frac{\tau_b}{a - a_c}, \quad \tau_0 \cong 2a_c\tau_1, \quad a_c = \frac{1}{3}(2\alpha)^{\frac{3}{4}} \quad (15)$$

The resulting long-time part of the single-site response and the correlation functions are

$$G(t) = \frac{2\alpha}{3a\tau_R} e^{-\frac{t}{\tau_R}}, \quad D(t) = \frac{2\alpha}{3a} e^{-\frac{t}{\tau_R}} \quad (16)$$

where  $\tau_R = 3\tau_1$ , and we see from (15,16) that the longest physical time-scale,  $\tau_R$ , diverges continuously at  $\Theta_G = -\frac{3}{2}(2\alpha)^{1/4}$  (cf. Fig. 1). At  $\Theta = \Theta_G$  the long-time part of  $D(t)$  shown in (16) becomes constant  $q = (2\alpha)^{1/4}$  showing that the Edwards-Anderson order parameter jumps at the  $\Theta_G$ . The resulting phase diagram is displayed in Figure 1; we note that  $T_G = (1 + \Theta_G)T_0$  occurs at a lower temperature than  $T_m$ , where the last low-temperature metastable states disappear [3] as discussed above.

The response function  $G(t)$  is a susceptibility with respect to the field conjugate to  $S = \exp i\phi$ , and thus cannot be measured directly. However, using  $G(t)$  found above, we can determine the ac-response to a time-varying physical magnetic field  $H(t)$  which is experimentally accessible. We focus on the total magnetic moment of the array generated by the Josephson currents:

$$\mathcal{M} = \frac{1}{2} \left( \frac{2e}{\hbar c} \right) l^2 \sum_{mn} \langle S_m \tilde{\mathcal{J}}_{mn} S_n \rangle \quad (17)$$

where  $\tilde{\mathcal{J}}_{mn} = imn\mathcal{J}_{mn}$  if  $m$  and  $n$  are indices referring to horizontal and vertical wires respectively. We would like to determine the response in this magnetization to a time-varying field; we use the fact that  $\mathcal{M} = 0$  for static  $H$  to write

$$\frac{\partial \mathcal{M}(t)}{\partial H(t')} = \left( \frac{2e}{\hbar c} \right)^2 l^2 \text{ReTr} \tilde{\mathcal{J}} \hat{G}(t, t') \tilde{\mathcal{J}} \hat{D}(t', t). \quad (18)$$

In order to evaluate (18) we will need the response function connecting wires of different type (horizontal/vertical)

$$\hat{G} = \hat{J} \frac{1}{\tilde{G}^{-2} - \beta^2 \hat{J}^\dagger \hat{J}} \quad (19)$$

and of the same type (cf. (8)). We use the Fourier representation of  $\hat{J}^\dagger \hat{J}$  and that of  $\hat{G}$  and  $\hat{D}$  to determine the ac-response,  $\frac{\partial \mathcal{M}(t)}{\partial H(t')}$ , in terms of the single-site response functions ( $L = Nl$ ):

$$\mathcal{M}(t) = \left( \frac{2e}{\hbar c} \right)^2 \left( \frac{L^2}{12} \right)^2 N \frac{J_0^2}{T} \frac{1}{\alpha^2} \left( 1 - \frac{J_0^2}{A^2 \alpha} \right) \int_{-\infty}^t G_{t-t'} D_{t-t'} [H(t) - H(t')] dt'. \quad (20)$$

We can insert the response and correlation functions found above to determine the ac susceptibility  $\chi_\omega = \frac{\partial \mathcal{M}_\omega}{\partial H_\omega}$  which leads to

$$\chi_\omega = - \left( \frac{2e}{\hbar c} \right)^2 \frac{2N}{9} \left( \frac{L^2}{12} \right)^2 \frac{J_0 \sqrt{\alpha}}{a} \frac{\omega}{\omega + 2i/\tau_R} \quad (21)$$

where  $\tau_R$  is the longest time-scale of the response:

$$\tau_R \approx \begin{cases} \frac{2\tau_b}{a(\Theta)} & \Theta > 0 \\ \frac{\tau_b}{a_c} \frac{|\Theta_G|}{(\Theta - \Theta_G)} & \Theta - \Theta_G \ll |\Theta_G| \end{cases} \quad (22)$$

$$a(\Theta) = \Theta + \sqrt{\Theta^2 + 2\alpha} \quad (23)$$

From Eq. (22) we see that the divergent relaxation times are directly observable in the physical a.c. magnetic response of the array. The zero frequency limit of the a.c. susceptibility jumps to a finite value at  $T = T_G$ , indicating the development of a finite superconducting stiffness at the transition. Therefore, the measurement of this a.c. response in a fabricated array serves as a probe of glass formation.

In summary, we have presented a periodic model which displays a dynamical transition where the system “freezes” into one of an extensive number of metastable states. Due to their large degeneracy, these states will not be selected by a Boltzman weight under equilibrium conditions. This glass transition at  $T_G$  is characterized by diverging relaxation times and by an accompanying jump in the Edwards-Anderson order parameter; the phase diagram of the array is displayed in Figure 1. It would be interesting to study the physical properties of this array below the glass transition temperature in its non-ergodic regime; in particular we expect “memory” effects in the form of an anomalous response function and “fingerprints” of the individual metastable states in its physical behavior. Since any uncertainty in the position of the wires introduces randomness in this array, it also offers the opportunity to study the crossover between glasses with spontaneously-generated and quenched disorder.

We thank D.M.Kagan for several useful discussions and for a careful reading of the text. M.V.F. acknowledges partial support from the International Science Foundation, the Russian Government (joint grant M6M300) and the Russian Foundation for Fundamental Research (grant #95-02-05720); M.V.F. and L.B.I. thank NEC Research Institute for hospitality.

- 
- [1] e.g. T.R. Kirkpatrick and D. Thirumalai, *PRB* **36**, 5388 (1987); J.P. Bouchaud and M. Mezard, *J. Phys. I* **4**, 1109 (1994); S. Franz and J. Herz, *PRL* **74**, 2115 (1995); M. Potters and G. Parisi, unpublished (cond-mat preprint 9503009) and references therein.
  - [2] e.g. E. Marinari, G. Parisi and F. Ritort, *J. Phys. A (Math. Gen.)*, **27**, 7647 (1994).
  - [3] P. Chandra, L.B. Ioffe and D. Sherrington, *Phys. Rev. Lett.*, **75**, 713 (1995).
  - [4] Strictly speaking the high-temperature expansions for  $D(t)$  and  $G(t)$  in (12) differ from those of the correlation and response function respectively; the former contain additional factors of  $(\beta^2 \mathcal{J}^\dagger \mathcal{J})$  that do not affect the long-time behavior near  $T_0$ .
  - [5] C. de Dominicis and L. Peliti, *Phys. Rev. B*, **18**, 353 (1978).
  - [6] H. Sompolinsky and A. Zippelius, *Phys. Rev. B*, **25**, 6860 (1982).
  - [7] V.M. Vinokur, L.B. Ioffe, A.I. Larkin and M.V. Feigelman, *Sov. Phys. JETP*, **66**, 198 (1987).